Synthetizing and Measuring Superconducting Sodium Cobalt Oxide (Na_xCoO_2) Crystals

Radosław Tomasz Chrapkiewicz

under the direction of
Prof. Young S. Lee
Massachusetts Institute of Technology

Research Science Institute
July 31, 2007

Abstract

Recently, the condensed matter physics community has been very interested in the new superconductor $Na_{0.3}CoO_2 \cdot yH_2O$. The superconducting mechanism is not known, and it is likely unconventional. Production of single crystal samples is difficult, and only a few groups in the world have produced them. In this paper, a general method for deintercalating Na from multiple crystals is developed. A superconducting crystal has been synthesized, and its physical properties have been measured. The chemical deintercalation method together with hydration in water instead of vapor was found to be a very fast, efficient method for creating small crystals samples.

1 Introduction

1.1 Superconductivity

The fundamental feature of superconductors is that their resistivity drops to zero below the critical temperature T_c. The phenomenon is caused by electron coupling (Cooper pairs) due to the electron–phonon interaction. A superconductor is a perfect diamagnet, repelling all magnetic fields from its interior. This Meissner effect exists below the critical field H_c for superconductors of type I. Fields above H_c destroy the superconductivity in the material. Similarly, currents higher than the critical current I_c destroy the superconducting phase. Type II superconductors also have zero resistivity and total field repulsion, but differ from the Type I in an important way. Above the critical field H_{c1} and below H_{c2}, we have the mixed state in which of magnetic field can penetrate the material. Above H_{c2} superconductivity is destroyed.

1.2 Na_xCoO_2

In 1997 sodium cobalt oxide with $x = 0.65 - 0.75$ was revealed as a material with unusual thermoelectric properties [1]. This material had high chemical stability and was non-toxic, making it a great candidate for many thermoelectric applications. That discovery prompted intensive research with Na_xCoO_2 .

In 1999 Ray *et al.* [2] discovered localized Curie–Weiss magnetism in Na_xCoO_2 , $x > 0.5$ materials. Curie–Weiss magnetism is similar to paramagnetism but with antiferromagnetic spin interactions. Until that time it was believed that the Curie–Weiss phenomenon appeared only in insulators, where magnetism is connected with the net spin of lattice ions. However, in the sodium cobalt oxide, Curie–Weiss magnetism coexists with metallic behavior. So far no theory has been developed to describe this phenomenon, motivating substantial research in recent years.

Properties of Na_xCoO_2 strongly depend on the sodium content (different phases presented in [3]). As previously mentioned, for sodium content $x > 0.5$ Na_xCoO_2 has Curie-Weiss metal properties. For $x < 0.5$, it behaves as an usual paramagnetic metal. Unique properties appear at $x = 0.5$, when this material becomes a charge–ordered insulator [4,5].

In 2004, Cava [3] proposed a phase diagram for Na_xCoO_2 . It was created on the basis of preliminary results but requires fully experimental confirmation for accuracy. The phase diagram for sodium oxide is presented in Figure 1 (from Foo *et al.* [3]).

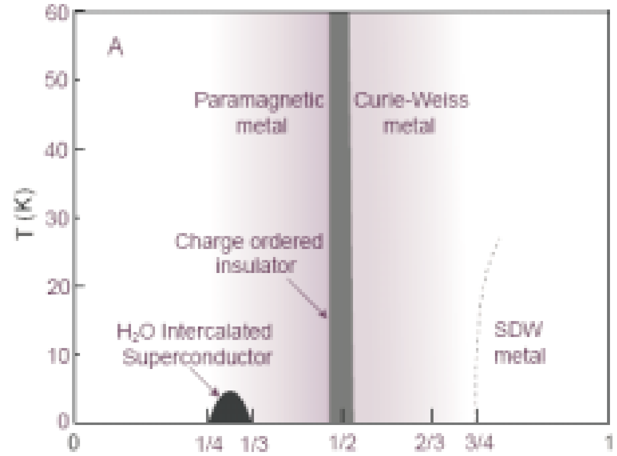

Figure 1: Phase diagram for Na_xCoO_2 . X label – x fractional number for sodium content. For initial samples $Na_{0.75}CoO_2$ we have antiferromagnetism phase (SDW metal).

1.3 Structure of Na_xCoO_2

The lattice of Na_xCoO_2 consists of two separated CoO_2 layers per unit cell. Between them there exists a sodium layer. Its structure strongly depends on the sodium content x and is not well defined. Each cobalt oxide layer forms an edge–sharing CoO_6 octahedral network. This structure is similar to that of high–T_c cuprate superconductors, except that in each layer the Co atoms form a triangular (hexagonal) lattice rather than a square lattice.

In a crystal of sodium content $x = 0.75$ at a temperature of 300 K the lattice constants (distances between ions) are equal to $a = 2.83$ Å and $c = 10.85$ Å. The lattice directions

a, b, c are marked in Figure 2 (Takada *et al.*(2003) [6]). Two kinds of cobalt ions appear in the lattice. There is a fraction $(1-x)$ of Co^{4+} with a spin $S = \frac{1}{2}$ and a fraction x with $S = 0$ Co^{3+} ions.

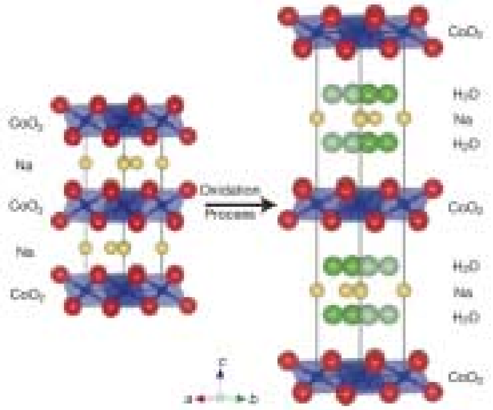

Figure 2: Structural views of $Na_{0.7}CoO_2$ (left) and $Na_{0.3}CoO_2 \cdot 1.4H_2O$ (right)

1.4 Superconductivity in Na_xCoO_2

Superconductivity in Na_xCoO_2 was discovered in 2003 by Takada *et al.* [6]. In Takada's studies superconductivity appeared in a sodium cobalt oxide with $x = 0.3$ after hydration. Water penetrates between cobalt oxide layers, separating them in the c direction without significantly influencing the a direction. This separation causes the environment for electrons to become "more two–dimensional", seemingly causing superconductivity. They showed that superconductivity appeared for $0.28 < x < 0.37$ with the critical temperature T_c between 4.3K and 4.8K [11] after sample hydration.

1.5 Objective

Understanding of the mechanism of superconductivity in $Na_{0.3}CoO_2 \cdot yH_2O$, which is similar in structure to high–T_c superconductors, is important for both fundamental physics and future technology. There have been many Na_xCoO_2 $0.25 < x < 0.33$ investigations studying powder samples. We aim to obtain a hydrated crystal sample with $x = 0.3$ ($Na_{0.3}CoO_2 \cdot 1.3H_2O$). The crystal state allows the anisotropic properties of the material to be examined. We use electrochemical and chemical method of sodium extraction. The first method used by Chou *et al.* [7] for similar studies, is likely to better control the sodium content in the crystal. The second method has been most widely used in preparing powder samples. There have not been many studies concerning $Na_{0.3}CoO_2 \cdot 1.3H_2O$ crystals, more investigation into their properties, in particular the anisotropic properties must be completed. By developing fast methods of obtaining samples we aim to intensify this area of material study. The magnetic properties of these crystals are also measured.

2 Experimental

The transformation of $Na_{0.75}CoO_2$ to $Na_{0.3}CoO_2$ was a crucial part of the experiment, since the material demonstrates superconducting properties for a narrow range around $x \simeq 0.3$.

2.1 $Na_{0.75}CoO_2$ crystals

We have used single crystals of $Na_{0.75}CoO_2$ grown in the Center for Materials Science and Engineering at MIT. Initially large samples are split into smaller $1-30$ mg irregular shaped pieces. The material was also very thin and brittle, prone to cleaving on the atomic plane *ab* during weighing or moving with tweezers. We were able to distinguish the *ab* plane on the microscope due to its smooth reflective surface [3].

2.2 Electrochemical deintercalation

Electrochemical de–intercalation was used because of its the ability to precisely control sodium content. It was proposed by Chou *et al.* [9] in 2004 during work on another superconductor La_2CuO_{4+y}. However, this method lasts longer and carries the possibility of additional reactions in the solution. Side reactions like the electrolysis of H_2O solution may influence the diagnostic measurements.

2.2.1 The principle of the reaction

In this method the following reaction governs the working electrode:

$$\mathrm{Na}_{0.75}\mathrm{CoO}_2 + \delta(\mathrm{OH})^- \longrightarrow \mathrm{Na}_{0.75-\delta}\mathrm{CoO}_2 + \delta(\mathrm{NaOH}) + \delta e^- \tag{1}$$

This reaction is favored due to the voltage difference between the surface of the sample and the electrolytic solution.

According to the reaction (1) we can use the number δ of electrons flowing through the circuit to find the sodium content $(0.75 - \delta)$. By time–integrate the current flowing through the counter electrode , we obtain the charge accumulate. Knowing the mass of the sample, we can determine coefficient x in Na_xCoO_2 .

2.2.2 Materials

Three–electrode electrochemical cells were set up. We have used 1 molar NaOH in D_2O solution. A three platinum-electrode system was used allowing us to control the potential between the reference electrode and the sample electrode (Figure 3).

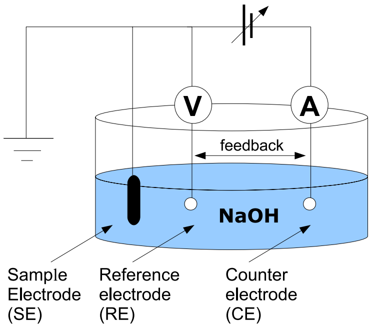

Figure 3: A three-electrode electrochemical cell

2.2.3 Controlling system

Two equivalent systems were used for controlling voltage between the reference electrode and the sample electrode . The first system involved *VoltaLab* hardware which could collect and record data on a computer. The second system, composes of circuits prepared by us, yielded more samples but with less precise control.

The four circuits were all designed to stabilize voltage between the reference and the sample electrode , and to measure currents and voltages without influencing conditions in the chemical cells. The circuit diagram is presented on Figure 4. The most important component of the circuit is the operational amplifier (LM741), whose main feature is linear amplification of the potential difference across its two legs. The configuration, shown in Figure 4 is a feedback circuit, with fluctuations of resistivity between the electrodes we compensated by variations in the CE potential. Moreover, capacitors in the circuits filter high frequency fluctuations.

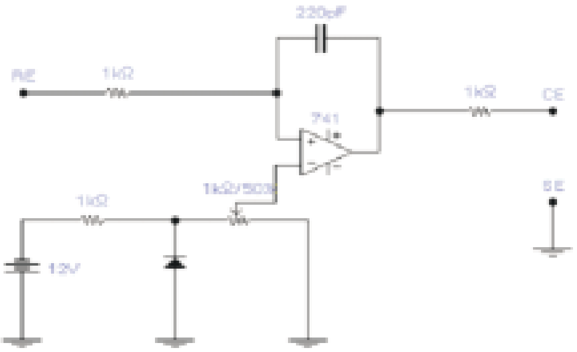

Figure 4: Circuit diagram for a feedback control circuit

Current and voltages were measured using a voltmeter, and results were recorded periodically. Time–Integration of current yielded an estimate of the charge accumulated as well as information about the sodium content in the sample.

2.2.4 Cyclic Voltometry scans

We wanted to have well defined voltage between between the sample electrode and reference electrode due to the counter electrode feedback. By changing voltage the reaction speed can be adjusted. On the other hand, higher voltages can cause other reactions in solution, and thus a loss of information about the de–intercalation progress.

The fastest way to determine the proper value of voltage is to identify the voltage–current characteristics for a cell via a cyclic voltometry scan. A voltage was periodically changed between -1V and 1V with constant speed equal to 10mV/s. The result of the CV scan is presented in the Figure 5. For electrolyte voltages higher than $\sim$ 600 mV, we observe rapid current increase connected with electrolysis appearance. The curve indicates the hysteresis feature of a CV scan caused by rearrangement of an ions distribution in the solution.

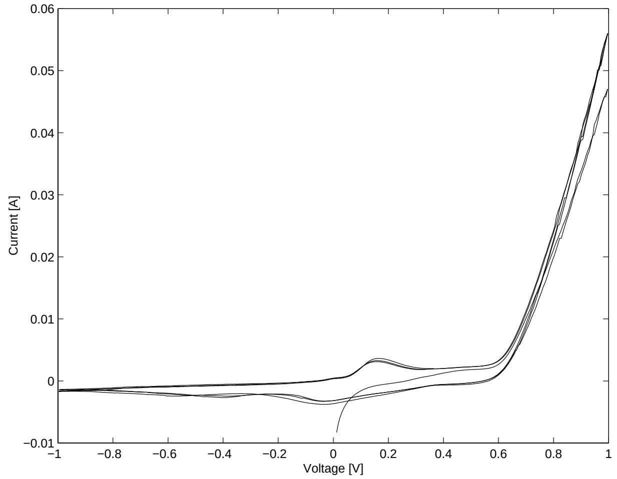

Figure 5: Cyclic voltometry measurements for the electrochemical cell

On the basis of Figure 5, we adjusted the proper voltage between RE and SE to 580 mV. Surprisingly, attempts with a voltage lower then 520 mV created an unwanted opposite current flow.

Ingredient	Amount
CH_3CN	100 mL
Liquid bromine	21.8 g
$Na_{0.75}CoO_2$ crystals	0.27 g

Table 1: Ingredients of the chemical reaction

2.3 Chemical sodium extraction

Additionally, we de–intercalated our samples via the following chemical reaction:

$$\mathrm{Na_{0.75}CoO_2} + 0.225\mathrm{Br_2} \rightarrow 0.45\mathrm{NaBr} + \mathrm{Na_{0.3}CoO_2} \tag{2}$$

Initially this method was used with Na_xCoO_2 powder. Transformation of the powder to $Na_{0.3}CoO_2 \cdot 1.3H_2O$ is much faster due to a large surface area, however, such a solution has many disadvantages. Powder samples do not demonstrate any anisotropic properties. The powder also does not seem to show a stable hydration phase. Although hydration is much faster in powder, due to a greater surface area, the superconducting phase disappears in a few minutes.

Using our chemical method we prepared small crystal samples using amounts of reagents as presented in Table 1. These are the amounts calculated to de–intercalated the powder samples. The reaction took place in a buffer of acetonitrile (CH_3CN). This is a good solvent bromine and has molecules which are too big to diffuse into the Na_xCoO_2 crystals.

We prepared 17 various size crystal samples (1mg−30mg) using this method de–intercalating them for 3 days.

2.4 Hydration

According to Takada (2003) [6], the superconducting phase in Na_xCoO_2 requires hydration, thus the prepared samples were placed in a very humid environment. In our case samples were sealed in plastic jars with damp cotton balls on the bottom. The jars were left in a room temperature environment for a few days. Each was placed sample lay on a platinum mesh allowing the vapor to diffuse from each side.

Although the method of hydrating samples with is quite successful (like in [7]), another method was also tested. Four samples were soaked in highly purified water for one day. This method was potentially dangerous for the samples, since liquid water may penetrate the crystal macro structure. If defects exist, internal tension is created and may eventually cause the crystal to break. Some defects were observed but the crystal was not broken into pieces. Also, this method may not have been faster because of the large surface tension of purified water. It means that the energy needed to move a water molecule from liquid to crystal phase may be too high. Despite these concerns, this method was attempted shown to lead to efficiently superconductivity.

2.5 SQUID measurements

We are mostly interested in the magnetic moments of our samples, their its dependence on field applied and their hysteresis. Measurements were performed using a Quantum Design MPMS–XL superconducting quantum interface device (SQUID).

2.5.1 Field cooling, measuring in zero–field applied and warming.

We have prepared very small samples ($1 - 30$mg) which are too small for direct resistivity measurements. Our proposed method allows zero resistivity phase measurement in a sample. We first cool a sample in a non–zero magnetic field and turn the field off. This results in rapid change in magnetic flux, inducing a circulating current in the sample. Assuming there is a superconducting phase, we should see a non–decaying, large magnetic moment caused by superconducting current. Upon warming the sample, there should be a rapid decrease of the observed magnetic moment which determines T_c.

However this is not the direct method of detecting a superconducting phase — measuring its zero resistivity using four–probe method. We cannot exclude a ferromagnetism phase which may cause a positive magnetic moment in zero field. When we combine this method with measuring hysteresis curves, the presence of a superconducting phase can be shown.

2.5.2 Cooling and measuring in set field

We can also detect a superconducting phase utilizing the Meissner effect. To avoid any influences form the samples sub–T_c history, we cool samples in a constant applied field. Afterwards, the sample is warmed and values of magnetic moment are recorded. We expect constant negative values for the magnetic moment below T_c. However, our samples have many impurities and may have not been uniformly de–intercalated and hydrated due to the short duration of the experiment. This results in an incompletely repelled field in the sample. Therefore we expect to get a significant decrease in the magnetic moment below T_c, but not necessarily constant negative values.

2.5.3 Zero field cooling. Measuring in the set field.

The principle of this method is to combine both of the methods presented in Sections 2.5.1 and 2.5.2. The sample is warmed in a constant field above the hypothetic critical temperature T_c and values of magnetic moment are recorded. Contrary to the method in Section 2.5.2, a sample is cooled below T_c in zero–field. Afterwards, we apply the magnetic field. Similarly to 2.5.1, we expect superconducting currents below T_c, this time resulting in a negative, diamagnetic signal.

2.5.4 Field–scan at constant temperature

For temperatures $T < T_c$, we can run the scan of magnetic moments for varying external fields. This method allows us to determine the type of superconductivity of the material and its critical fields. For the superconductors of type II like $Na_{0.3}CoO_2 \cdot yH_2O$, we expect linear decrease in moment for fields $0 - H_{c1}$. For $H = H_{c1}$ we should observe the lowest value of magnetic moment of the sample. Between H_{c1} and H_{c2} there should be increase of the value. As it was mentioned in Section 2.5.2 we do not necessarily expect negative values due to the sample impurities.

2.5.5 Hysteresis curve

We have also performed hysteresis curve measurements. Even though we expect either superconducting or paramagnetic material, hysteresis curves are used to prove the existence of a non–ferromagnetic phase using the procedure in Section 2.5.1. Measurements took place under constant temperature with only the applied magnetic field changing.

3 Results

3.1 Samples from the electrochemical cells

Manual measurements with the controlling system along with *VoltaLab* measurements yielded gave results which the estimation of the level of sodium extraction. Integration of the current flowing through the counter electrode yielded the total accumulated charge and therefore (from the reaction given in Equation (1)) information on the amount of deintercalation that had occurred. Although we have assumed that no other reactions interfered, diagnostic susceptibility measurements showed that we had been managed to obtain a sodium content $x \simeq 0.5$. A plot of magnetic susceptibility χ is presented in the Figure 6. Comparing to Chou *et al.*(2004) [10], we recognize anomalies in susceptibility at 53 K and 88 K characteristic of the phase transitions in $Na_{0.5}CoO_2$. This and other results show that all of our samples demonstrate $Na_{0.5}CoO_2$ properties. We attempted to make Na_xCoO_2 with $x < 0.5$ but were unsuccessful. This indicates the existence of some

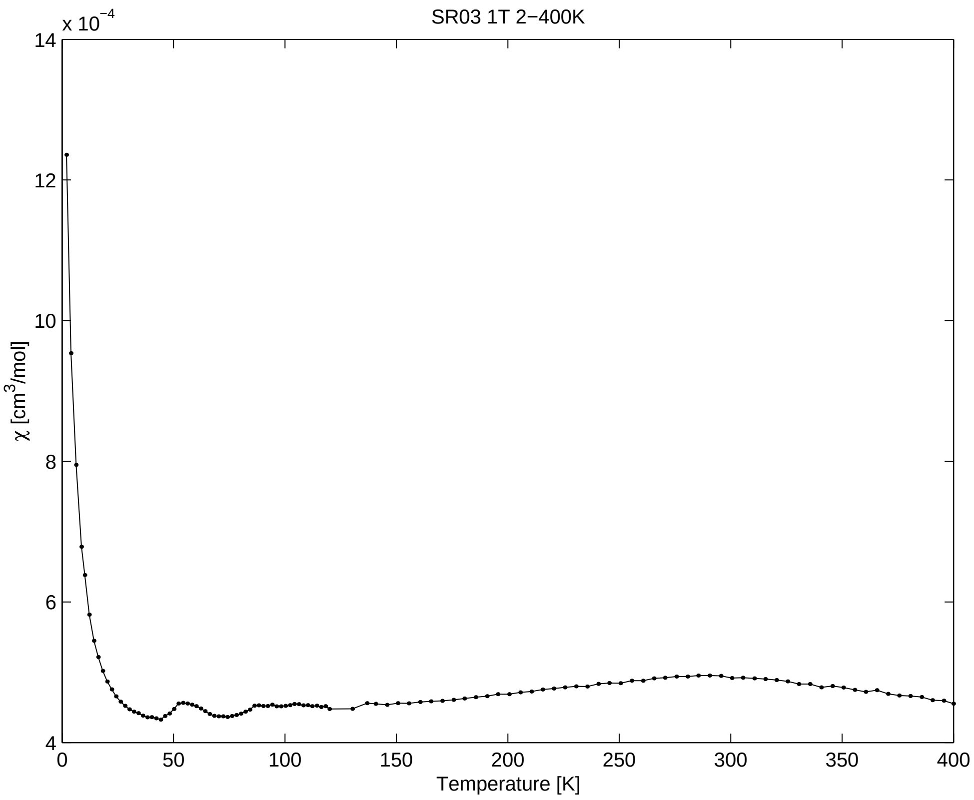

Figure 6: $\chi(T)$ for the sample from electrochemical de–intercalation. Mass of the sample $m = (4.7 \pm 0.2)$ mg

side reactions in the solution, and that the voltage between the electrodes was to high.

3.2 Crystals obtained using chemical de–intercalation

The chemical method turned out to be a much more efficient and faster method than the electrochemical method. We have succeeded in obtaining a superconducting crystal which was hydrated via immersion in purified water.

3.2.1 Na_xCoO_2 with $x \simeq 0.3$

In Figure 7 we present a magnetic susceptibility curve for the sample with mass $m = 33 \pm 0.2$ mg after three–days of chemical deintercalation. Compared to Figure 6, there are no peaks characteristic of $Na_{0.5}CoO_2$, resulting in a curve similar to that of $Na_{0.3}CoO_2$ from Chou *et* *al.*(2004) [10]. We observe at least three different phases of material that occur at temperatures of $2-100$ K, $100-300$ K and $300-400$ K. The first may be connected with either Curie–Weiss magnetism or paramagnetism, the second with weak antiferromagnetism interactions (breaking with the temperature), and the last with paramagnetism. However, more studies with comparisions to theoretical predictions are needed to determine all of phase transitions in this material.

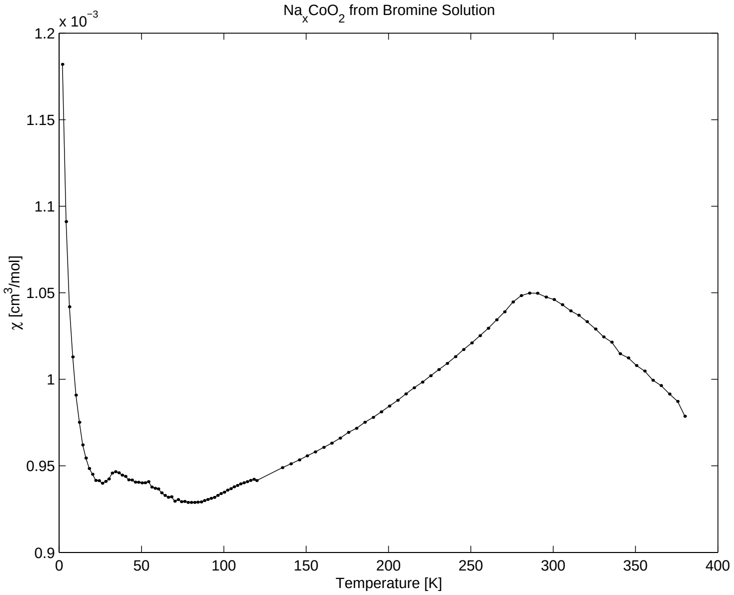

Figure 7: Sample from bromine solution. Assumed de–intercalation to $Na_{0.3}CoO_2$

3.2.2 $Na_{0.3}CoO_2 \cdot yH_2O$

We observed superconducting phase evidence in the crystal of mass $m = 28.1 \pm 0.2$ mg. The crystal was hydrated for one day and entirely immersed in purified water. From Chou *et al.*(2004) [7], we expected a superconducting phase below 5 K with a field of 20 Oe below H_{c1}. We determined the critical temperature for our material to be $T_c = 2.6 \pm 0.15K$.

Meissner effect — set field cooling and measuring We performed the method described in Setion 2.5.2 in a 20 Oe field. We expect to see a rapid decrease in the magnetic moment of the sample due to the Meissner effect. In Figure 8 we present a plot of magnetic moment versus temperature. Positive values are due to a non–superconducting areas and impurities in the material. However, we see that below $\sim$ 3K there is the rapid decrease caused by the repulsion of the magnetic field from the interior of the superconducting areas in the sample.

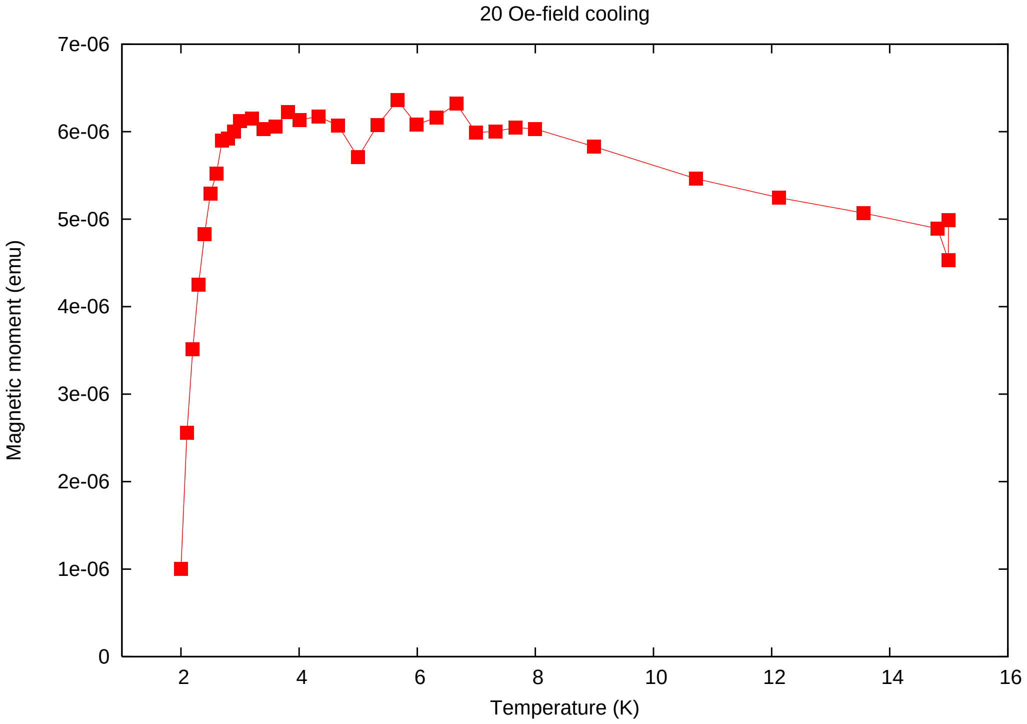

Figure 8: The drop of magnetic moment below T_c caused by the Meissner effetct.

Cooling in non–zero field and turning off the field More evidence for superconducting phase is presented in the Figure 9. We performed the SQUID measurement method proposed in section 2.5.1. The rapid decrease of the sample magnetic field from 20 Oe to $\sim$ 0 Oe suggests the presence of macro phenomenon such as a superconducting current (connected with zero resistivity) in the entire sample and the micro–trapping of magnetic vortexes on impurities [8]. Furthermore, hysteresis curves did not display ferromagnetic features, excluding this phase and proving the existence of superconductivity in the sample.

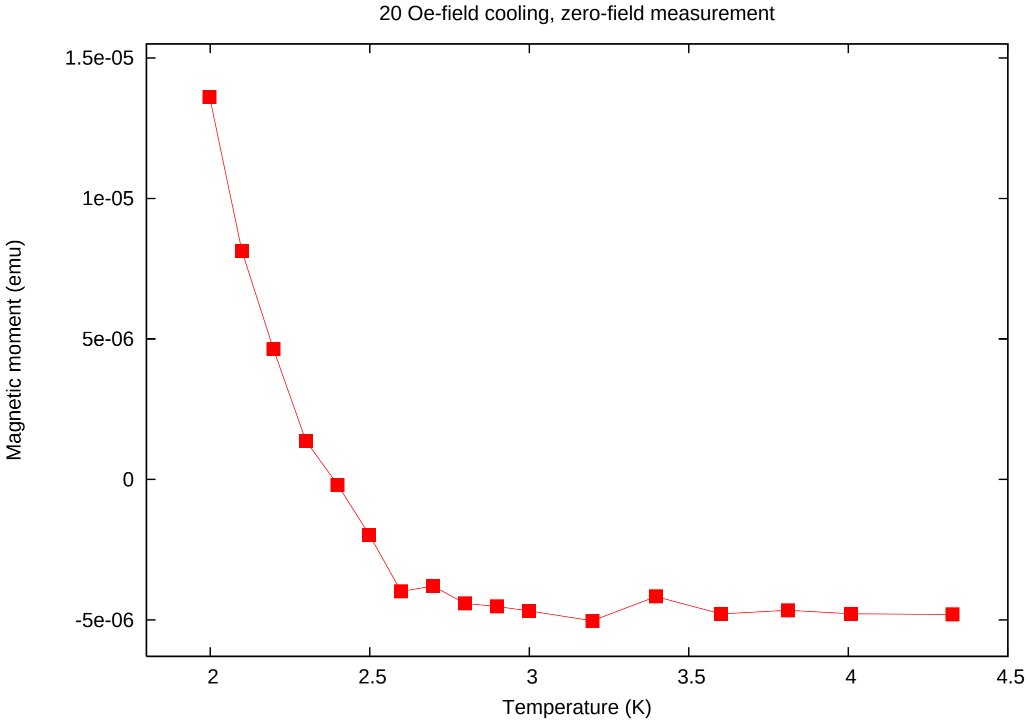

Figure 9: The magnetic moment below T_c caused by induced superconducting currents in the sample.

Zero field cooling The last method described in Section 2.5.3 was expected to give very negative values for the magnetic moments of sample due to the positive increase in the external field. In fact such negative values have been measured. A plot of the magnetic moment is presented in the Figure 10(a). The moment value abruptly drops at a temperature of $\sim$ 3K. More precise measurements are presented in Figure 10(b) with a temperature range $2 - 4$K showing that $T_c \simeq 2.6$K.

3.2.3 $\mathrm{Na}_{0.3}\mathrm{CoO}_2 \cdot y\mathrm{H}_2\mathrm{O}$ four days after hydration

Four days after hydration (2 days after the first series of measurement), we repeated measurements describeed in Section 2.5.2 (Figure 10) for the same sample. Suprisingly we

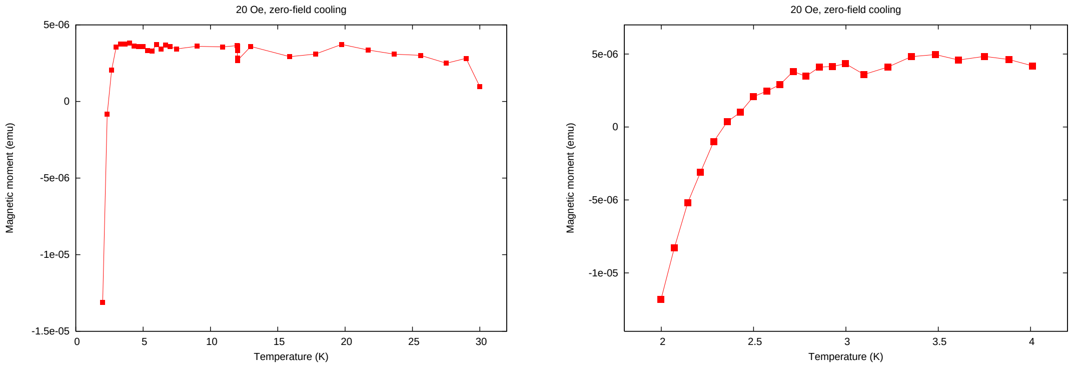

(a) Sample cooled in 0 Oe fiels, measured in 20 Oe field. Significant negative moment caused by superconducting currents in the sample.

(b) The precise measurement of range 2–4K from the Figure 10(a)

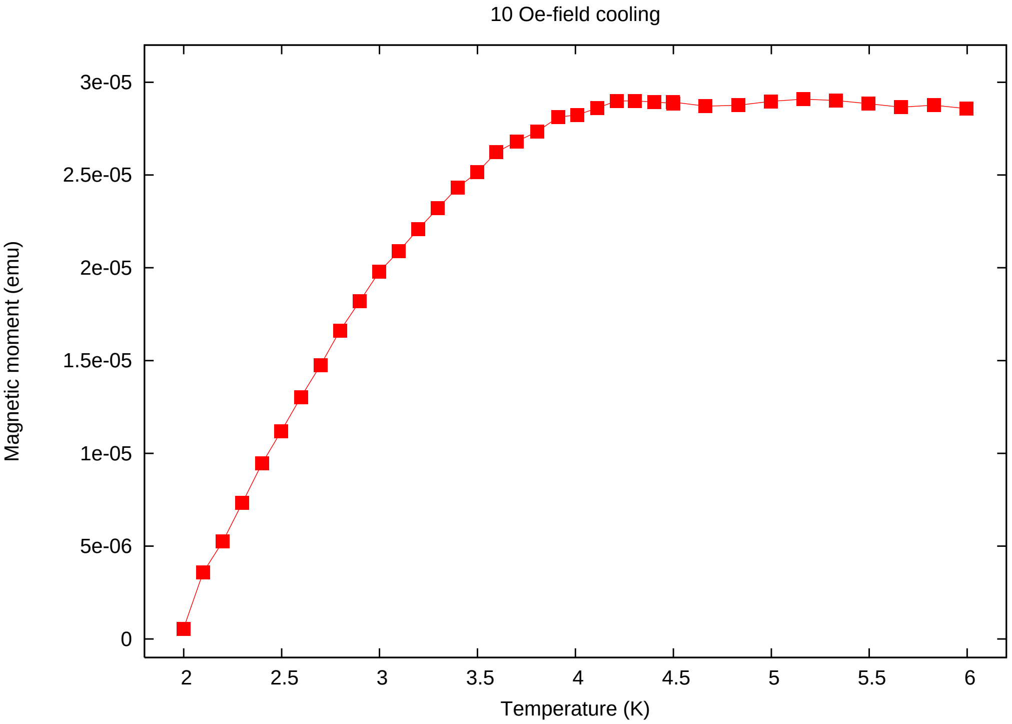

Figure 10: The Meissner effect. We observe the new $T_c \simeq 4.2$ K

obtained a higher critical temperature $T_c \simeq 4.2$ K. It was probably caused by diffusion of H_2O from the surface to the sample interior. Seemingly more uniformly hydrated samples exhibit stronger superconductivity properties.

3.3 Conclusion

Results presented in this work demonstrate the existence of superconductivity below $T_c =$ 4.2K in the synthesized crystal. However, on the basis of the method in Sections 2.5.3 and 2.5.1, according to the initial measurements, we see that a magnetic moments are not constant below T_c as was expected . This observation might be caused by slightly different properties in some areas in the crystal as well as thermal excitation of the Cooper pairs.

The low T_c does not allow us to classify $\mathrm{Na_{0.3}CoO_2 \cdot }y\mathrm{H_2O}$ as a high-T_c superconductor. However, due to the similar 2–D lattice character and half spin (S=1/2) of the ions in the lattice, the mechanism of the superconductivity in this material may be similar. Therefore further studies of crystal behavior should be performed.

Finally, this method takes 5–6 days to weak crystal samples $<$ 30 mg as opposes to a couple of months for other methods. Although the presented method produces smaller crystals, it is useful for quick investigations.

4 Acknowledgments

I would like to thank my mentor Prof. Young S. Lee, for making it possible for me to work in his labs, for answering all of my questions, and for providing with background information. I would also like to thank Michael Sneella for instructing me in experimental techniques, building electronic circuit, and lab protocol. I wish to thank Dr. Shaoyan Chu from the Center for Materials Science and Engineering for assistance and advice regarding the chemical de–intercalation process. I wish to thank Dr. Chris Akerman, my tutor for patience in correcting my paper, advising me and for all of his help during the writing process. I wish to thank Prof. Lee's graduate students, and the people who helped me to write this paper — TA's, especially Johann Komander, RSI participants and alumnis.

Especially I would like to acknowledge Mr. Ryszard Rakowski of the Polish Children's

Fund and the Center of Excellence in Education for giving me the unique chance to participate in the Research Science Institute.

References

[1] I. Terasaki, Y. Sasago, and K. Uchinokura. Large thermoelectric power in $NaCo_2O_4$ single crystals. Physical Review Letters B 56, R12685 (1997).

[2] R. Ray, A. Ghoshray, and K. Ghoshray. ^{59}Co NMR studies of metallic $NaCo_2O_4$ Physical Review Letters B 59, 9454 (1999).

[3] M. L. Foo, Y. Wang, S. Watauchi, H. W. Zandbergen, T. He, R. J. Cava, and N. P. Ong. Charge–ordering, commensurability and metallicity in the phase diagram of layered Na_xCoO_2 . Physical Review Letters 92, 247001 (2004).

[4] H. W. Zandbergen, M. Foo, Q. Xu, V. Kumar, and R. J. Cava. Sodium ion ordering in Na_xCoO_2 : Electron diffraction studyPhysical Review Letters B 70, 024101 (2004).

[5] Q. Huang, M. L. Foo, J. W. Lynn, H. W. Zandbergen, G. Lawes, Yayu Wang, B. H. Toby, A. P. Ramirez, N. P. Ong, and R. J. Cava. Low temperature phase transitions and crystal structure of $Na_{0.5}CoO_2$. Journal of Physic: Condensed Matter 16, 5803 (2004).

[6] K. Takada, H. Sakurai, E. Takayama–Muromachi, F. Izumi, R. A. Dilanian, and T. Sasaki. Superconductivity in two-dimensional CoO_2 layers. Nature 422 (2003), 53–55.

[7] F.C. Chou, J. H. Cho, P. A. Lee, E.T. Abel, K. Matan, and Y. S. Lee. Thermodynamic and Transport Measurements of Superconducting $Na_{0.3}CoO_2 \cdot 1.3H_2O$ Single Crystals Prepared by Electrochemical Deintercalation. Physical Review Letters 92, 157004 (2004).

[8] C. P. Poole, H. A. Farach, R. J. Creswick. *Superconductivity.* Academic Press, San Diego, California (1995).

[9] F. C. Chou, E. T. Abel, J. H. Cho, and Y. S. Lee. Electrochemical De–intercalation, Oxygen Non–stoichiometry, and Crystal Growth of $Na_xCoO_{2-\delta}$. cond-mat/0405158, (2004)

[10] F. C. Chou, J. H. Cho, and Y. S. Lee. Magnetic susceptibility study of hydrated and nonhydrated $Na_xCoO_2 \cdot yH_2O$ single crystals. Physical Review Leters B 70, 144526 (2004).

[11] C. J. Milne, D. N. Argyriou, A. Chemseddine, N. Aliouane, J. Veira, S. Landsgesell, and D. Alber. cond-mat/0401273, (2003).

[12] Stephen K. Lower *Electrochemistry.* 1994/03/08.

[13] D. R. Garcia. *Investigation of Superconducting and Non-Superconducting Phases of* $Na_{0.3}CoO_2 \cdot 1.3H_2O$. B.A. thesis, Massachusetts Institute of Technology, Cambridge, MA (2004).